The Tomographic Approach to Ground Penetrating Radar for Underground Exploration and Monitoring

Michele Ambrosanio, *Member, IEEE*, Martina T. Bevacqua, *Member, IEEE*,
Tommaso Isernia, *Senior Member, IEEE*, Vito Pascazio, *Senior Member, IEEE*

***Abstract*— The underground exploration and characterization via non-destructive imaging approaches is paramount for the modern scientific community. The reason of such a great interest is related to the wide range of applications this analysis is involved in, which spans from the civil engineering world until to the archaeological and forensic fields, and planetary explorations.**

In this framework, ground penetrating radar (GPR) is becoming one of the leading technologies due to its flexibility and ease of application, as it can be employed in different configurations and environmental conditions. Standard GPRs provide a user-dependent map of the underground and subsurface targets, known as "radargram", whose interpretation requires a firm human expertise. Moreover, this technology does not allow, in its standard version, to infer about the nature of the targets buried below the soil, unless some a priori information is available.

Aim of the work is to provide some guidelines to explore and move through the huge variety of conventional and unconventional approaches employed in the framework of underground exploration in order to underline the advantages deriving from the use of the more recent tomographic techniques, which can improve considerably the quality of the recoveries.

***Index Terms*— ground penetrating radar, subsurface imaging, inverse scattering, non-linearity, regularization techniques.**

I. Motivation

THE topic of non-invasive and non-destructive exploration of the soil has proved to be of great interest for the scientific community over the last years [1]. As a matter of fact, many efforts from several disciplines have been devoted to the development of systems able to provide a reliable scan of the subsurface objects buried below the ground, as well as on the development of advanced techniques and processing able to improve the accuracy and reliability of the retrieved information. In this framework, ground penetrating radar (GPR) is nowadays considered as one of the most powerful underground non-destructive monitoring tools. Over time, this technology witnessed great development within several different fields of application spanning from demining to lunar explorations, and including glaciology, archaeology, geology, and, of course, civil engineering [1-3].

Generally, it is an application-dependent technology, whose hardware and electronics are relatively variable according to the aim of the considered analysis. It represents an active technology based on radar systems which work by radiating an electromagnetic pulse into the ground and by measuring the strength of the echoes produced by the interactions with the buried structures. This one-dimensional (1-D) recording can be moved to a two-dimensional plot (2-D), known as radargram, by changing the antenna location and determining the echo-delay time (which is related to the depth coordinate) versus the radar position.

Despite the ease and fast processing of the standard operation mode, the generated map is hard to be interpreted, as shown in Fig. 1. As a matter of fact, an expert user and the availability of some a priori information regarding the domain under investigation are mandatory for a reliable interpretation. Moreover, this simple processing is able to survey only the presence and location of buried objects, but not their characteristics, unless some additional a priori information is provided. Furthermore, it can lead to misleading results in more complicated scenarios due to the assumption that the velocity of the investigating wave is constant, which is not realistic for many scenarios.

Therefore, more user-friendly, complete and convenient approaches are desirable in order to improve the quality of subsurface analyses. From this point of view, tomographic approaches can play a very relevant role [4]. These techniques aim at providing images of the buried objects and/or information regarding the variations of dielectric permittivity and conductivity profiles of the scene under investigation. Accordingly, image formation requires an accurate modeling of the scattering phenomena in order to properly take into account the complex interactions among sources, receivers, ground and buried objects. However, the development of robust and

This is the postprint version of the following article: M. Ambrosanio, M. T. Bevacqua, T. Isernia and V. Pascazio, "The Tomographic Approach to Ground-Penetrating Radar for Underground Exploration and Monitoring: A More User-Friendly and Unconventional Method for Subsurface Investigation," in *IEEE Signal Processing Magazine*, vol. 36, no. 4, pp. 62-73, July 2019. doi: 10.1109/MSP.2019.2909433. Article has been published in final form at: https://ieeexplore.ieee.org/document/8746870.

TABLE I
QUALITATIVE PERFORMANCE ASSESSMENT IN GPR PROCESSING [6].

IMAGING PERFORMANCE	Horizontal resolution	$\approx \frac{\lambda_{sec}}{2 \sin \theta_{emax}}$
	Vertical resolution	$\approx \lambda_{sec}$
DATA REQUIREMENTS	Spatial sampling	$= \frac{\lambda_{smin}}{4 \sin \theta_{emax}}$
	Time sampling	$= \frac{1}{B_{int}}$
	Frequency sampling	$\leq \frac{c_0}{2b\sqrt{\varepsilon_{sr}\mu_{sr}}}$

θ_{emax}: maximum effective view angle (assumed symmetrical);
λ_{sec}: effective central received wavelength in the soil;
λ_{smin}: minimum wavelength in the soil for the selected bandwidth;
c_0: speed of light in the vacuum;
b: length of the two-dimensional imaging domain;
ε_{sr}: relative permittivity of the soil;
μ_{sr}: relative permeability of the soil;
B_{int}: bandwidth of interest (after signal filtering).

reliable recovery algorithms still has some issues related to both modeling errors as well as the presence of uncertainties on the data.

The proposed paper aims at underlying the importance of the tomographic approaches in the framework of the under-ground exploration of the soil by exploiting a GPR technology. The main approaches to the solution of this problem will be considered in order to highlight the advantages deriving from their use.

II. GPR SYSTEMS: TECHNICAL REQUIREMENTS AND LIMITATIONS

There are essentially two kinds of GPR systems which are available for commercial and experimental devices: pulsed and stepped-frequency ones. A pulsed system radiates and receives the echoes deriving from the transmitted electromagnetic pulse. On the other hand, a stepped-frequency GPR decomposes the electromagnetic pulse into its spectral components and radiates them sequentially as a train of monochromatic sinusoidal signals [5].

Due to the soil properties, which can be assumed as time-invariant within the time needed for the GPR measurement campaign, both the pulsed and stepped-frequency systems can be considered equivalent from a theoretical point of view. In practice, although the pulsed GPR is quite common in commercial devices and it has been employed for a longer time, the stepped-frequency GPR technology has been claimed more performing.

A key role in GPR systems is played by the frequency bandwidth and the spatial and frequency resolutions [5]. Regarding the frequency bandwidth, it depends on the considered application, and a sketchy classification can be provided. Generally, low frequencies (below 200 MHz) are employed for depths that overcome 5-7 meters or more (e.g., in some geological applications), radio frequencies (200 – 700 MHz) for applications where the depth to be reached is of the order of 3 m (e.g., some archeological prospecting), higher

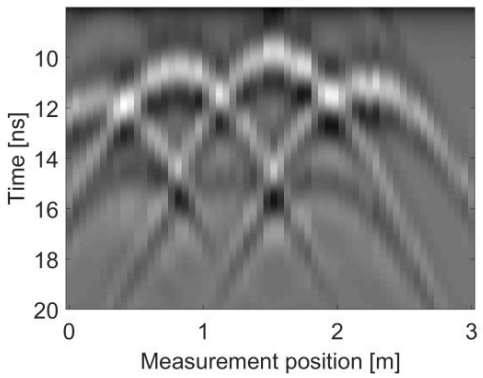

Fig. 1: Two-dimensional conventional "radargram" with several buried scatterrers.

radio frequencies (700 – 3000 MHz) for applications where the maximum required investigation depth can be limited to the order of 1 m (e.g., detection of fractures and asphalt monitoring) [5]. Finally, even higher microwave frequencies can be employed where the maximum investigated depth can be limited to the order of 50 cm (e.g., demining) [6].

Concerning spatial resolution, it is quite hard to find a general analytic expression. Nevertheless, under some simplifying assumptions, such as in the diffraction tomography case, it is possible to obtain an order of magnitude for these quantities [6]. The evaluation of the spatial resolution proposed here is referred to the capability of distinguishing two "equally strong" scatterers at the same depth/lateral coordinate, giving a qualitative measure of resolution in both directions, assuming that both targets scatter the same energy. Table I reports also some qualitative formulas regarding the suboptimal spatial, temporal and frequency sampling for the GPR data sampling. More details regarding the quantities involved in Table I can be found in [6], not reported here for the sake of brevity.

III. GPR DATA PROCESSING

Different acquisition modalities are available. In the simplest one, the GPR data are collected relatively to a single spatial point versus the time coordinate, which is labelled as A-scan. The comprehensive set of GPR traces pertaining to an entire scanned line is referred to as B-scan, which corresponds to a matrix of values reporting scanning spatial positions versus time. It is equivalent to assume that the GPR system stops in each A-scan position for the acquisition, gathers the data in that position, and moves on the next one (both a continuous mode as well as "stop-gather-and-go-on" acquisition modalities can be employed). Finally, the acquisition of GPR data relative to a series of parallel B-scans is usually named as C-scan.

Thus, the collected data, usually called raw data, if adequately processed, can allow target identification, but in general the formed image and its interpretation can be improved considerably after suitable pre- and post-processing. Indeed, GPR system is heavily contaminated by clutter and its reduction represents a key objective. The clutter usually is related to the part of signal which is not due to the buried target, that is the field reflected by medium interfaces as well due to antenna

coupling, and so on. A key factor in clutter removal techniques is represented by the medium interfaces. Indeed, neglecting the electromagnetic interaction between antenna and the soil interface can become a limiting factor for detecting targets close to it [7]. This is related to the fact that the echoes scattered back from the air-ground interface present relatively high amplitudes, which may mask small objects shallowly buried. Filtering these first interface reflections by incorporating in scattering model the incident near-field distribution transmitted in the soil by the antenna can cancel the undesired reverberation effects and further improve the imaging results. Moreover, since the roughness profile of the interface separating the air from the ground is generally unknown, it could be useful to estimate the surface profile before the characterization of the buried targets by means of a pre-processing of the collected data [8, 9].

When two or more antennas are simultaneously used, another source of deterministic clutter is represented by the direct coupling between antennas, so that some techniques have been introduced to take into account this aspect [10, 11].

The processing of GPR data represents a large topic for the signal processing community. In particular, two fundamental categories of processing can be identified, i.e. deconvolution-based [12] and tomographic imaging approaches [6]. In the former, one essentially processes the single GPR traces by taking advantages from a simplified Fourier based model. The latter is usually concerned with a processing that regards all the traces within a B-scan or a C-scan and is aimed to focus within a vertical plane (2D models) or in a buried volume (3D models) the targets embedded in the host medium at hand.

Fig. 2 shows a clear comparison between these two classes. It is clear that if the electric size of involved scatterers is small, then good recovery performance can be achieved exploiting both methods. But when moving to the realistic case of extended objects, the conventional deconvolution-based approaches fail, as they do not take into account the strong non-linearity of the physical interactions among the scatterers; conversely, the tomographic approach manages to improve the detection performance considerably.

Within this class, there is a plethora of models and related algorithms which have been developed in a context wider than that of the GPR data processing and belongs to the literature of microwave scattering, which is the physical mechanism underlying the tomographic approaches [13].

IV. The Inverse Scattering Problem

In the following, the mathematical formulation of inverse scattering problems is introduced in more details with respect to the general 3D scalar case by assuming and dropping the time harmonic factor $exp\{j\omega t\}$. Moreover, for the sake of simplicity, non-magnetic media are considered and the magnetic permeability is assumed everywhere equal to that of free space μ_0. This assumption is quite realistic for most soils and targets involved in the GPR framework.

A simple 3D sketch of a tomographic microwave imaging system for GPR applications is reported in Fig. 3. The scenario is composed of two media: the medium 1 (usually the air) represents the region where the probes are located, while the medium 2 (the soil) is the region wherein one wants to investigate. The non-magnetic unknown object-of-interests are located inside the imaging domain (ID) Ω in the medium 2, and their electrical properties are denoted with $\varepsilon_s(\boldsymbol{r})$ and $\sigma_s(\boldsymbol{r})$, being $\boldsymbol{r} = (x, y, z) \in \Omega$ the coordinates of the reference system. The relative permittivity and the electrical conductivity of the ID are identified by $\varepsilon_b(\boldsymbol{r})$ and $\sigma_b(\boldsymbol{r})$, respectively.

The aim of the GPR inverse scattering problem consists of retrieving the unknown contrast function $\chi(\boldsymbol{r})$, which relates the electromagnetic features of the objects to the ones of the host medium. This function is defined mathematically as:

$$\chi(\boldsymbol{r}) = \frac{\varepsilon_s(\boldsymbol{r}) - j\sigma_s(\boldsymbol{r})/\omega\varepsilon_0}{\varepsilon_b(\boldsymbol{r}) - j\sigma_b(\boldsymbol{r})/\omega\varepsilon_0} - 1, \tag{1}$$

where $\omega = 2\pi f$, and f is the working frequency. To this end, the region of interest is probed by means of receiving/transmitting radar antennas located on a measurement surface Γ above the interface at given height.

The two fundamental equations describing the relevant GPR imaging problem for a given generic incident field $\boldsymbol{E}_i$ are the state equation and the data equation. The mathematical expressions of these latter, in case of non-magnetic media are, respectively [13]:

$$\boldsymbol{E}_{\mathrm{t}}^{(v)}(\boldsymbol{r},\omega) = \boldsymbol{E}_{\mathrm{i}}^{(v)}(\boldsymbol{r},\omega) + \int_{\Omega} \boldsymbol{G}_{\mathrm{i}}(\boldsymbol{r},\boldsymbol{r}',\omega)\chi(\boldsymbol{r}',\omega)\boldsymbol{E}_{\mathrm{t}}^{(v)}(\boldsymbol{r}',\omega)\,\mathrm{d}\boldsymbol{r}', \quad \boldsymbol{r},\boldsymbol{r}' \in \Omega \tag{2.a}$$

$$\boldsymbol{E}_{\mathrm{s}}^{(v)}(\boldsymbol{r},\omega) = \int_{\Omega} \boldsymbol{G}_{\mathbf{e}}(\boldsymbol{r},\boldsymbol{r}',\omega)\chi(\boldsymbol{r}',\omega)\boldsymbol{E}_{\mathrm{t}}^{(v)}(\boldsymbol{r}',\omega)\,\mathrm{d}\boldsymbol{r}', \quad \boldsymbol{r} \in \Gamma \tag{2.b}$$

where $v = 1, \ldots, N_v$, identifies the v-th different illuminations (or views) of the imaging system, and $\boldsymbol{E}_{\mathrm{i}}$, $\boldsymbol{E}_{\mathrm{t}}$, $\boldsymbol{E}_{\mathrm{s}}$ are the incident electric field inside Ω, the total electric field inside Ω, and the scattered electric field measured on a domain Γ in medium 1, respectively. $\boldsymbol{G}_{\mathrm{i}}$ and $\boldsymbol{G}_{\mathbf{e}}$ are the internal and external dyadic Sommerfeld-Green functions, which represent the impulse response observed inside and outside the imaging domain Ω, respectively, by an elementary source located inside Ω. Assuming by the sake of simplicity a homogeneous soil, one can use the Sommerfeld-Green functions pertaining to the so-called "half-space" configuration [6].

Eqs. (2) need to be treated an solved, so after a proper discretization of domain Ω in integrals (2.a) and (2.b), which involves the discretization of $\chi(\cdot)$ and $\boldsymbol{E}_{\mathrm{t}}(\cdot)$, unknown and state of the GPR problem [14], and after choosing a proper number of different measurement points for the scattered field $\boldsymbol{E}_{\mathrm{s}}$, data of the problem [4], it becomes, neglecting the view index v for sake of simplicity:

$$\boldsymbol{z} = \boldsymbol{e}_i + \mathbf{A}_i(\boldsymbol{x} \odot \boldsymbol{z}) = \boldsymbol{e}_i + \mathbf{A}_i^{\mathbf{x}}(\boldsymbol{z}), \quad \text{in } \Omega \tag{3.a}$$

$$\boldsymbol{y} = \mathbf{A}_e(\boldsymbol{x} \odot \mathbf{z}) + \boldsymbol{n}, \quad \text{on } \Gamma \tag{3.b}$$

where the elements of vector $\boldsymbol{x}$ represent the unknown contrast χ, $\boldsymbol{e}_i$ is the vector which samples the incident known field $\boldsymbol{E}_{\mathrm{i}}$, $\boldsymbol{z}$ is the vector which samples the total unknown field $\boldsymbol{E}_{\mathrm{t}}$ (the state), $\boldsymbol{y}$ is the vector which samples the scattered electric field $\boldsymbol{E}_{\mathrm{s}}$ on Γ (data of the problems), $\mathbf{A}_i$ and $\mathbf{A}_e$ are the discrete

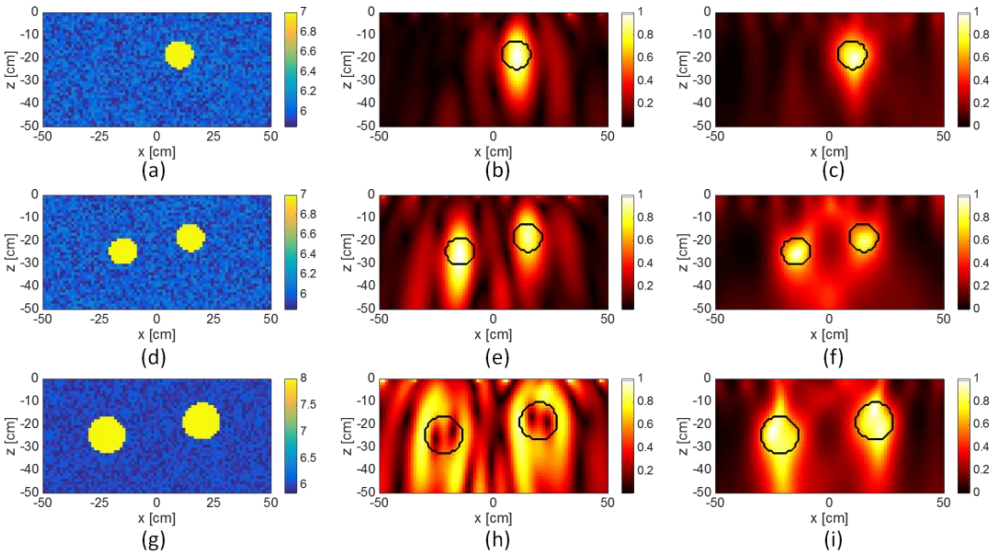

Fig. 2: Comparisons between deconvolution-based and tomographic imaging approaches in a 2D framework. (a)-(d)-(g) Permittivity of the reference profiles. Qualitative reconstructions via the former (b)-(e)-(h) and the latter (c)-(f)-(i) approaches. In the last example, the size of the objects is increased and the strong non-linearity limits the inversion performance of standard methodologies seriously.

counterparts of integrals in Eqs. (2.a) and (2.b), and $\boldsymbol{n}$ is the unavoidable additive measurement noise, here considered white and Gaussian. Operation "$\odot$" denotes the element-by-element product between the two vectors $\boldsymbol{x}$ and z, and $\mathbf{A}_i^{\boldsymbol{x}}[(\cdot)] = \mathbf{A}_i[\boldsymbol{x} \odot (\cdot)]$.

Solving eq. (3.a) for z, and substituting it in eq. (3.b), we obtain the final unknown-data equation:

$$\mathbf{y} = \mathbf{A}_e(\boldsymbol{x} \odot (\mathbf{I} - \mathbf{A}_i^{\boldsymbol{x}})^{-1}\boldsymbol{e}_i) + \boldsymbol{n} = \boldsymbol{T}_{\boldsymbol{e}_i}(\boldsymbol{x}) + \boldsymbol{n} \qquad (4)$$

where $\mathbf{I}$ is the identity operator. The explicit dependence of the of discrete operator $\boldsymbol{T}_{\boldsymbol{e}_i}$, on the incident field $\boldsymbol{e}_i$ wants to stress that the link between the noisy measured scattered field samples $\boldsymbol{y}$ and the unknown contrast $\boldsymbol{x}$ is dependent also on how one can choose incident fields, involving waveform design: how many, how different (position, frequencies, …), etc.

The GPR imaging inverse problem, through the inversion of discrete operator $\boldsymbol{T}_{\boldsymbol{e}_i}$, aims at retrieving the unknown $\boldsymbol{x}$ from the knowledge of the noisy data $\boldsymbol{y}$. Such a problem is non-linear respect to $\boldsymbol{x}$, and is ill-posed. The former circumstance descends from the dependence of the total field $\boldsymbol{z}$ on the unknown contrast $\boldsymbol{x}$ expressed by the state equation (3.a) [13], while the latter from the compactness of the radiation operator $\mathbf{A}_e$, as described in the following sections.

These difficulties are further worsened when, as in subsurface sensing, it is not possible to probe the targets from all the different directions, thus reducing the amount of available data and entailing an unavoidable deterioration of the imaging results. On the other hand, although commonly exploited in monostatic configuration, in order to increase as much as possible the essential dimension of data and to improve the performance of the inversion tomographic strategy, GPR systems in multiple-input-multiple-output (MIMO) configurations can be exploited.

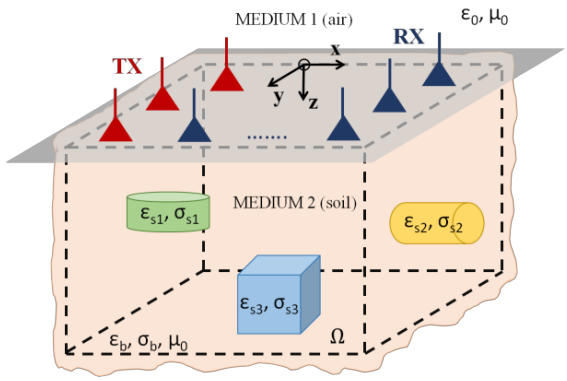

Fig. 3: Three-dimensional geometry of the subsurface imaging problem.

V. The Intrinsic Loss of Information in Inverse Scattering

The forward scattering problem implies a certain loss of information on the unknown contrast, and this implies that one can seldom retrieve exactly the actual ground-truth. From a theoretical point of view, one can exactly say the problem is ill-posed. In order to understand this concept, it is better to define what a *well-posed* problem is. According to Hadamard's definition [13], a problem is well-posed if it satisfies *all* the following three conditions:

- the solution exists;
- it is unique;
- it depends continuously on the data.

If at least one of the previous conditions is not fulfilled, then

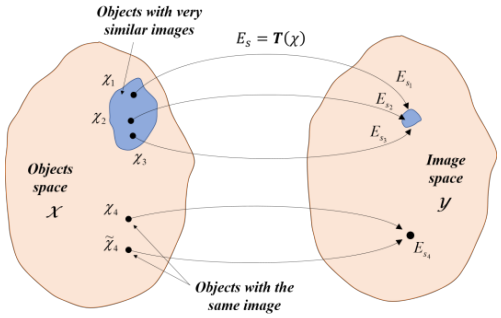

Fig. 4: Ill-posedness of the inverse scattering problem. Different objects χ can share the same images E_s or images which are very similar, due to the low-pass filtering properties of the scattering operator $\boldsymbol{T}$.

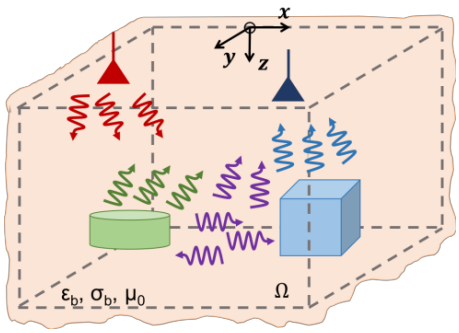

Fig. 5: Sketch of the physical meaning of the non-linearity.

the problem is named ill-posed. In order to understand properly the meaning of an ill-posed problem, it is important to define the class of objects to be imaged. This space is usually denoted as "object space", and each element of it is associated with one element of another space, called the "image space", by means of the forward problem, whose solution represents the link between these two spaces. A brief sketch is shown in Fig. 4.

Due to the loss of information deriving from the properties of the operators in Eq. (4), two or more objects might have the same image, or images very close to each other, and this results in the ill-posedness of the inverse problem at hand. Moreover, due to the unavoidable presence of noise on data and the failure of the third Hadamard's condition, small modifications of (measured) data will involve jumps in the solution. The above circumstances might drive into completely meaningless solutions from a physical point of view. Thus, there is a strong need to find efficient and reliable regularization strategies [13] to restore the well-posedness of the inverse problem and to obtain stable generalized solutions.

VI. Non-Linearity

From a physical point of view, in inverse scattering, non-linearity stems from multiple interactions between scattering objects and/or parts of them (see Fig. 5).

From a mathematical point of view, as discussed in the previous section, the radiator operator is compact, then it is not possible to invert the data equation and substitute it in the state equation. On the contrary, one can only invert the state equation and substitute in the data equation, giving rise to eq. (4). It is worth by observing eq. (4) that even though $\mathbf{A}_i$ and $\mathbf{A}_e$ discrete operators themselves are linear, the relation between the scattered field $\boldsymbol{y}$ (data) and the contrast function $\boldsymbol{x}$ (unknown) given by $\boldsymbol{T}_{\boldsymbol{e}_i}$ is non-linear. According to the above considerations, a generalized solution to inverse scattering is usually looked for by seeking the global minimum of [13]:

$$\Phi(\boldsymbol{x}) = \sum_{v=1}^{N_v} \eta^{(v)} \left\| \boldsymbol{y}^{(v)} - \boldsymbol{T}_{\boldsymbol{e}_i^{(v)}}(\boldsymbol{x}) \right\|^2, \tag{5}$$

where the explicit dependence on the different views has been restored, $\|\cdot\|$ is the ℓ_2 norm, and $\eta^{(v)}$ are normalization coefficients.

An alternative approach involves the simultaneous solution of the system of equations (3.a)-(3.b) for both the contrast $\boldsymbol{x}$ and the electric fields inside Ω. By so doing, a price is paid as the set of unknowns enlarges, but the degree of non-linearity reduces to that of a fourth order polynomial. In this case, the problem is generally solved by seeking the global minimum of:

$$\begin{aligned}\Phi\left(\boldsymbol{x}, \boldsymbol{z}^{(1)}, \cdots, \boldsymbol{z}^{(N_v)}\right) \\ = \sum_{v=1}^{N_v} \left\{ \eta_e{}^{(v)} \left\| \boldsymbol{y}^{(v)} - \mathbf{A}_e[\boldsymbol{x} \odot \mathbf{z}^{(v)}] \right\|^2 \right\} \\ + \sum_{v=1}^{N_v} \left\{ \eta_i{}^{(v)} \left\| \boldsymbol{z}^{(v)} - \boldsymbol{e}_i{}^{(v)} + \mathbf{A}_i^{\boldsymbol{x}}[\boldsymbol{z}^{(v)}] \right\|^2 \right\},\end{aligned} \tag{6}$$

where $\eta_e^{(v)}$ and $\eta_i^{(v)}$ are two normalization coefficient sets for the data and state equations, respectively.

Due to the non-linearity of the underlying problem, both the cost functionals (5)-(6) are non-quadratic ones, so that it may have several local minima which are "false solutions" of the problem (see Fig. 6). The more the problem departs from a linear one, the more the occurrence of false solutions. As a consequence, the obtained results depend on the considered initial guess.

Several strategies do exist to tackle and defeat the occurrence of the false solutions. Next section underlines these main strategies and proposes a brief discussion regarding their advantages and limitations.

VII. Solution Methods

Even if the solution of an inverse scattering problem does not represent a trivial task, the achievable performance can be really impressive with respect to the one obtainable with deconvolution-based approaches, as witnessed in experimental results shown Fig. 7 and reported in [15]. A natural question then arises on how one can obtain the results in Fig. 7 and which inversion techniques are available. Nowadays, most of the tomographic approaches present in the literature for the solution of the above discussed problem can be classified into three main categories:

- **qualitative methods**, which aim at detecting the scatterers hosted in the ID and retrieving only a limited

amount of information, that are scatter location and shape. They usually trade the reduction of the achievable information, with the absence of approximation and with a low computational burden;

- **approximated methods**, which adopt some approximations of the scattering phenomena that allow to simplify the mathematical model and to speed up the processing and reduce the computational complexity;
- **non-linear quantitative methods**, which aim at retrieving both electrical and morphological properties of the ID, by tackling the inverse scattering problem (3) in its full non-linearity, without involving any approximations and by minimizing a cost functional, such as (5) or (6). The main practical drawback is the long (or extremely long) reconstruction times required in order to complete the minimization.

A further class of minimization strategies includes hybrid approaches, which are usually based on a first qualitative step which aims at providing some rough information, which is then exploited in the next quantitative steps to avoid false solutions and to allow reliable and effective recoveries.

Fig. 8 provides a raw, qualitative classification of the solution approaches according to their estimated computational burden.

A. Qualitative methods

Qualitative methods aim at solving the inverse obstacle problem, which consists in reconstructing only the support of the unknown targets by processing the fields they scatter. Usually, these methods achieve the support information in a simple and effective way by working with exact models of the scattering phenomenon or by considering an auxiliary linear problem thus avoiding the difficulties related to the solution of the original (non-linear) inverse problem.

Many different qualitative strategies have been developed in literature. Among them, the most popular category of qualitive methods are the *sampling* methods [16], which are valid for both dielectric and metallic targets. They identify the spatial support of the scatterer by computing an indicator function over an arbitrary grid of points which samples the scenario under investigation. This indicator function will assume very different values, depending on whether they are evaluated within or outside the scatterer's support. As a consequence, by identifying a fixed threshold, one can discriminate between point inside and outside the targets. The linear sampling (LSM) and factorization (FM) [16] methods belong to this class of inversion algorithms. They require a multistatic/ multiview/ single-frequency configuration but can be extended to the case of multifrequency data by a posteriori combining the results from single frequency data.

Other approaches [17, 18] to get the shape of an obstacle amounts instead at solving corresponding *inverse source* problem, which aims at recovering the induced currents, defined as $\boldsymbol{w} = \boldsymbol{x} \odot \mathbf{z}$, from the knowledge of measured scattered field. These latter are based on the evidence that,

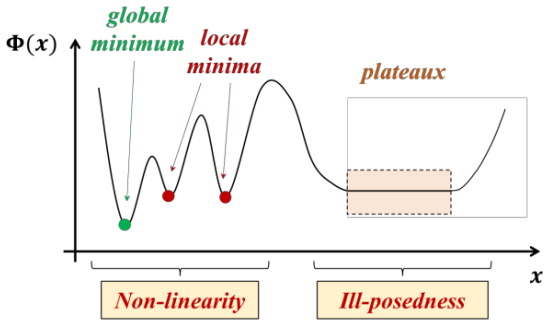

Fig. 6: Pictorial representation of a generic monodimensional cost functional with main issues in inverse scattering problems.

whatever the performed scattering experiments, the support of the induced currents is exactly equal to the one of the unknown scatterer. By so doing, the problem could be dealt with as a linear one by just inverting equation (3.b). However, such inverse source problem is severely ill-posed, as many different contrast sources can produce the same scattered field. To overcome such a difficulty, it has been recently argued that some decisive profit can be gained by enforcing some expected properties on the currents and proper coherence relationships among the currents pertaining to each performed scattering experiment. To this end, approaches in [17, 18] profitably introduce the enforcement of joint sparsity, while approach in [18] also benefits from equivalence principles to deal with dielectric objects.

When the targets have been already detected and their dielectric properties are known and constant, the qualitative characterization of the buried obstacle can be pursued by an iterative process based on a level-set formulation [8]. In this formulation, the problem is reduced to an optimization scheme where just the shape of the scatterer is looked for and the full non-linearity of the problem is considered. The algorithm involves the use of a level-set function in order to represent the boundary of the obstacle.

The simultaneous detection and localization of multiple targets can be also pursued via time-reversal (TR) based approaches, which include TR imaging (TRI), decomposition of reverse time operator (DORT) and time reversal multiple signal classification (MUSIC) [19]. The TRI is the most direct and intuitional method for target localization, which is based on the reverse of the field in time domain (or phase-conjugated in frequency domain) would precisely retrace the path of the original wave back to the source where it is excited thus determining the target's position. As such, the imaging resolution is constrained to the diffraction limit. Moreover, in case of multiple scatterers TRI focuses more strongly on the dominant scatterer and masks the weaker scatterers, while the imaging process is very time consuming. DORT and TR-MUSIC overcome these problems by exploiting the singular value decomposition of the multistatic response matrix, whose elements are defined as the scattered field detected at the different receiver due to the excitation of the transmitters. In particular, the signal and null space of the response matrix are

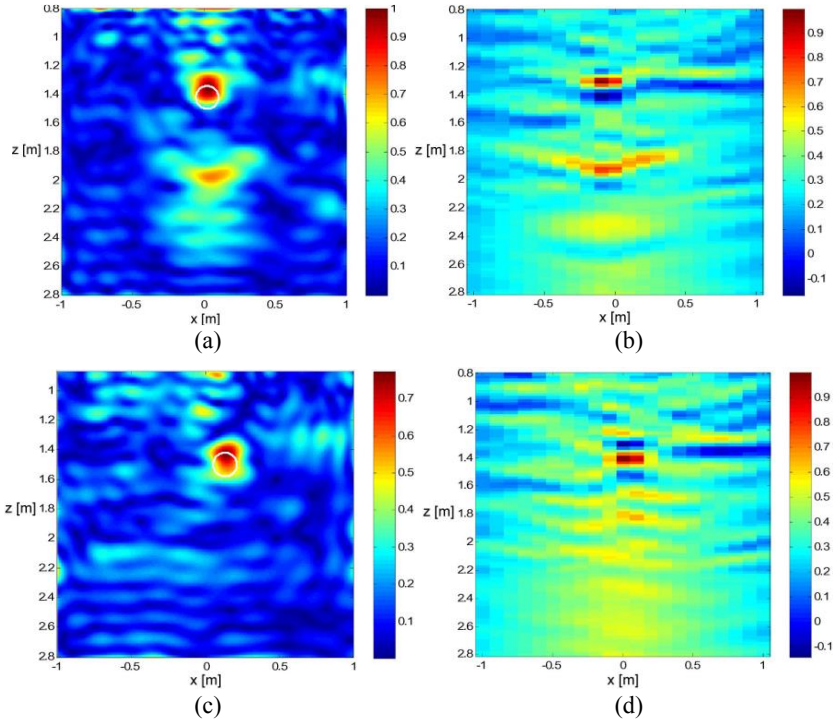

Fig. 7: Two-dimensional experimental reconstructions of the normalized amplitude of the contrast function for dielectric buried pipes. Water-filled case, tomographic (a) and migration-(c) approaches; air-filled case, tomographic (b) and migration-(d) approaches. Courtesy of Pettinelli et Al. [15].

used in order to define DORT and TR-MUSIC pseudo-spectrums, respectively. With respect to DORT and TRI, TR MUSIC became very popular, because it is not only algorithmically efficient but also capable to achieve a resolution that can be finer than the diffraction limit [19].

B. Approximated methods

As a countermeasure to non-linearity, *approximated* methods allow a very easy implementation and require a limited amount of computer memory and computational time, even though they suffer from several limitations induced by the adopted *approximated model*.

The most popular approximation of the scattering model (3) is the Born Approximation (BA) [10, 20]. In BA, the inverse scattering problem is linearized as the auxiliary unknown total field inside the object is assumed equal to the incident field. This hypothesis is fully satisfied only in absence of the object itself so that the BA is acceptable in case of weak scatterers, i.e., for objects whose internal characteristics are very close to the ones of the hosting medium, and/or for objects whose dimension is very small in terms of the wavelength in the external medium.

Other examples of approximated methods is the physical optics approximation or Kirchhoff approximation (KA) [21]. The KA can be adopted in case of scattering from electrically large perfect electric conductors. Under such a linear approximation, the solution algorithm is formulated as the inversion of a linear integral operator who relates the scattered data to a distributional unknown function that is directly related to the illuminated boundary of the object. Therefore, the inversion allows to retrieve targets' support.

Another relevant linearized approach has been introduced in the last years within the virtual scattering experiments (VE) framework [14]. The approach is based on a proper linear combination of the original incident (in Ω) and corresponding scattered fields (on Γ), in order to introduce new (virtual) experiments. In particular, the VE design is pursued in such a way to condition the scattering phenomena and enforce a circular symmetry on the total field. Then, a novel approximation to effectively linearize the scattering problem, even in the case of non weak scattering regime, is introduced. The range of applicability significantly outperforms the usual BA, as the VE based approximation is target dependent and considers the contribution of the field scattered by the object.

As improvement with respect to the above discussed linearized methods on the quadratic method [22] is also worth being mentioned. In this latter, a weak degree of non-linearity is introduced by adopting a second order approximation for the unknown-data mapping operator. In subsurface prospection the multiple interactions between scattering objects and/or parts of them occur inside a lossy medium. This circumstance allows to take into account just for the first order internal mutual interaction to adequately approximate the scattered field inside Ω. With respect to the linear methods, as for instance BA, it allows to reconstruct a wider class of unknown profiles.

Another interesting and efficient inversion method which goes beyond the limitations introduced with the BA has been proposed in [23], by exploiting a higher-order extended Born

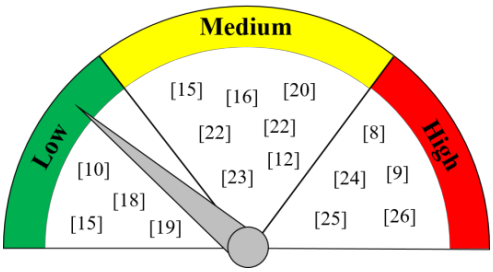

Fig. 8: Qualitative measure of computational complexity of the main solution methods.

approximation to reconstruct the conductivity function of dielectric objects buried in a lossy soil.

It is important to underline that the aforementioned approximated methods are quantitative, i.e. can give the full characterization of the targets, as long as the adopted approximated model holds true. Saying it differently, they are not able to provide an accurate description of the targets' features when exploited outside the range of validity of the underlying approximations, although they may provide some interesting qualitative results. [10].

C. *Non-linear Quantitative methods*

Non-linear quantitative approaches allow to widen the class of retrievable objects considerably at the expense of a higher computational burden and longer processing time, and the occurrence of local minima in the minimization procedure, which may drive into false solutions. As a consequence, their convergence is guaranteed only when the initial step belongs to the attraction basin of the solution, which can be hardly estimated.

In this class, an estimate of the contrast function is obtained through iterative procedures. Since there is no guarantee of avoiding false solutions unless a sufficiently accurate starting guess (i.e., a trial solution close to the global optimum) is available, global optimizations might represent valid tools thanks to their capability to explore the solution space by escaping from local minima [24]. Unfortunately, their complexity exponentially grows up with the number of unknowns: the more unknowns are considered, the higher their computational burden is [13].

In order to bypass the limitations related to the use of global minimization approaches, some algorithms exploit a local optimization framework. Examples of the approaches belonging to this class can be grouped into two main families: the first group, the Newton-Kantorovich (NK) approaches, tries to solve Eqs. (3) by minimizing the function in (5), while the second class, known as modified-gradient (MG) class, handles the electromagnetic inverse scattering problem at hand by re-arranging both the state and data equations in a single functional minimization (as reported in Eq. (6)) [25].

Distorted Born iterative methods [26] belongs to the first class and aims at solving the two coupled scattering integral equations via a succession of linear problems to update the internal fields and Green's function. The so called contrast source inversion scheme belongs to the second class. It tackles the problem by minimizing the functional (6) and by considering the currents induced inside the objects as auxiliary unknowns (rather than the total fields). Opposite to field-type approaches, one of the two fundamental equations of the electromagnetic scattering, i.e. the Eq. (3.b), becomes linear, thus reducing the overall non-linearity of functional (6).

VIII. Regularization Strategies

Exploiting a regularization technique is equivalent to add some *a-priori* information to the problem at hand in order to compensate the loss of information implicit in the direct problem and restore the well-posedness. Such *a-priori* information cannot be derived from the data or from the properties of the mapping which relates data and unknowns, but it is something strictly related to the expected properties of the contrast function χ to be retrieved. The effectiveness of the different regularizations will depend on how much the unknown scenario 'fits' the regularization model.

The simplest form to enforce some a *priori* information is to include a regularizing term $\Phi_R(\boldsymbol{x})$ in the cost functionals (5) or (6). Indeed, such additive term will allow to construct from the beginning a solution both compatible with the data (within the experimental error) and which exhibits the specific physical features. The additional information which can be exploited and/or enforced includes (but it is not limited to):

1. a requirement on the energy of the solution such as for instance a minimum l_2 energy requirement. This is the case of the well-known Tikhonov regularization technique [13];
2. a piecewise constant behavior on the contrast function [14];
3. physics induced bounds on the values of the unknown permittivity and conductivity functions (f.i., positive conductivities).

The main issue in such a kind of regularization strategies is related to the choice of the regularization parameters, i.e. the weight assigned at each $\Phi_R(\boldsymbol{x})$ term, whose selection is a crucial and critical point. As a matter of fact, no simple and general rules exist to perform such a choice in an optimal way.

While adding a penalty term is probably the most popular way of enforcing the regularization, there are of course other ways. Among the others, a possible strategy amounts to introduce proper statistical tools, such as in [27], in which a Markov-random-field approach based on maximum-a-posteriori estimation method is proposed by the authors, which showed better performance also when compared with conventional techniques like Tikhonov regularization [13].

Another alternative is that of keeping the dimensionality of the unknowns' space low by adopting a suitable (convenient) basis to represent the unknown function, that is:

$$\boldsymbol{x} = \mathcal{P}(\hat{\boldsymbol{x}}), \tag{7}$$

in which $\mathcal{P}$ represents the considered projection operator, $\hat{\boldsymbol{x}}$ represents the lower-dimensional representation of the contrast function in the selected imaging domain. In fact, a necessary (still not sufficient) condition to overcome ill-posedness is that the dimension of the space where the unknown function is looked for is not greater than the one of the data space. Such a

strategy is usually referred to as 'regularization by projection'. As far as the choice of the projection operation is concerned, a great interest is covered by Wavelet decomposition. Indeed, the wavelet basis offers the possibility to decompose the unknown profile into two sets of coefficients, namely coarse and detail coefficients, thus allowing intrinsic multiresolution representation of the unknown.

A similar idea is adopted in multiresolution regularization techniques [4],[24]. These regularization techniques allow to accommodate the representation coefficients for the contrast unknowns in a non-uniform fashion within the investigated domain. The reason for which this feature is quite interesting is twofold: first of all, on the basis of some a priori information, it is possible to focus the processing only in those regions where the scatterers are located, and secondly, a variable degree of resolution is expected with different depths, as in the GPR case, by exploiting a coarser resolution for the deeper parts of the investigated domain and preserving a higher number on unknowns for the shallower regions [24].

In order to restore the well-posedness of the problem, another interesting opportunity is offered by the *sparsity* regularization techniques, which are based on the concept of sparsity, i.e the possibility to represent this latter through a limited number of nonzero coefficients of a convenient basis. Provided the proper expansion of the unknown is used, such techniques guarantee that an accurate retrieval of the unknown is possible even for a number of data much lower than the overall number of basis coefficient, but sufficiently larger than the number of nonzero elements. Note that sparsity regularized techniques are well developed and understood for the case of phenomena described through linear models, hence, they are usually exploited in conjunction with linearized model (see the section VII.B), which are usually referred to as *sparse linear regression model*. This latter has been an active research area for the signal processing community for several decades and different algorithms have been introduced in signal processing community, which can be roughly divided into three main categories: greedy search heuristics, iterative re-weighted linear least square, and l_p-regularized methods.

The widely used methods are probably the last ones, which estimatesthe regression coefficients by minimizing a l_p-regularized least square objective function [25]:

$$\Phi_p(\boldsymbol{x}) = \|\boldsymbol{y} - \mathbf{L}\boldsymbol{x}\|_{l_2}^2 + \lambda\|\boldsymbol{x}\|_{l_p}^p , \qquad (8)$$

where the constant $\lambda > 0$ is the regularization parameter and $\mathbf{L}$ represents the linear(ized) GPR operator relating data (i.e., the scattered field samples $\boldsymbol{y}$) to the unknowns (i.e., the contrast function $\boldsymbol{x}$), and "p" is a parameter between 0 and 1.

With the advent of *compressive sensing*, a great attention has been paid to (8) by the signal processing community when $p = 1$. The theory of compressed sensing has shown that under sparsity and incoherent assumptions, solving the l_1-minimization problem is equivalent to solve the l_0-minimization problem, i.e. Eq. (8) when $p = 0$ (where the limit is taken in the sense of [28, 29], which amount to count the number of non-zero elements).

Even though the l_1-minimization is convex (which is the key advantage over the pseudo l_0 norm), it is still a challenging problem to be solved due to the size of the system matrix and non-differentiability of the objective function. To circumvent this issue, different iterative algorithms have been proposed that are based on linear programming or interior-point methods [28, 30]. However, these algorithms tend to suffer for computational burden and inaccuracy of the solution. As a consequence, faster approaches have been proposed aiming at overcoming these limitations via speeding-up and parallelizable strategies [29].

The concept of sparsity has been further explored along the years in the signal processing community, since additional sparse structure in the form of non-zero elements can be analysed. An interesting example is represented by a type of sparsity which is referred to as group-sparsity or block-sparsity or joint sparsity, in which the nonzero elements are arranged in clusters that allows to achieve better reconstruction results than just treating the signal as being arbitrarily sparse [17, 18]. More in detail, joint sparsity can be taken into account via mixed l_2/l_0 norm [17], which is normally utilized to count the number of nonzero blocks. Moreover, it can be also enforcing by defining an auxiliary variable as shown in [18].

IX. Conclusion

This contribution aims at helping researchers, engineers and all the readers to have a first look and understanding of tomographic approaches for non-invasive and non-destructive exploration of the soil by means of GPR.

With respect to standard GPR data processing, which requires human expertise and may show high probability of false alarms, tomographic approaches allow to obtain images that are more reliable and readable, as shown in the previous sections. However, such approaches involve the solution of an inverse scattering problem, that does not represent a trivial task. In the scientific literature, different methods to overcome the difficulties of the inverse scattering problem underlying tomographic approaches have been proposed.

The choice of the best solution and regularization approach is up to the application and to the available a priori information. For instance, if the aim is just the detection of buried objects, qualitative methods, such as LSM or MUSIC, should be exploited. On the other hand, if one is also interested on object characterization (e.g., stone, mine or other), by paying a price in terms of computational burden, quantitative methods and in particular iterative non-linear methods can be adopted.

The efforts of the scientific community for the incoming future will be devoted to develop faster and more reliable inversion strategies for the detection as well as characterization of the buried targets. Such an aim will require as mandatory step the use of hybrid approaches which combine the advantages of different methods coming from various disciplines, spanning from signal processing to other engineering fields.

References

[1] A. Benedetto and L. Pajewski, *Civil engineering applications of ground penetrating radar*. Springer, 2015.

[2] L. B. Conyers, *Ground-penetrating radar for archaeology*. AltaMira Press, 2013.

[3] X. Feng and M. Sato, "Pre-stack migration applied to GPR for landmine detection," *Inverse problems,* vol. 20, no. 6, p. S99, 2004.

[4] O. M. Bucci, L. Crocco, T. Isernia, and V. Pascazio, "Subsurface inverse scattering problems: quantifying, qualifying, and achieving the available information," *IEEE Transactions on Geoscience and Remote Sensing,* vol. 39, no. 11, pp. 2527-2538, 2001.

[5] A. C. Gurbuz, J. H. McClellan, and W. R. Scott, "A compressive sensing data acquisition and imaging method for stepped frequency GPRs," *IEEE Transactions on Signal Processing,* vol. 57, no. 7, pp. 2640-2650, 2009.

[6] R. Persico, *Introduction to ground penetrating radar: inverse scattering and data processing*. John Wiley & Sons, 2014.

[7] E. Cristofani, M. Becquaert, S. Lambot, M. Vandewal, J. Stiens, and N. Deligiannis, "Random Subsampling and Data Preconditioning for Ground Penetrating Radars," *IEEE Access,* 2018.

[8] O. Cmielewski, H. Tortel, A. Litman, and M. Saillard, "A two-step procedure for characterizing obstacles under a rough surface from bistatic measurements," *IEEE Transactions on Geoscience and Remote Sensing,* vol. 45, no. 9, pp. 2850-2858, 2007.

[9] T. U. Gurbuz, B. Aslanyurek, E. P. Karabulut, and I. Akduman, "An efficient nonlinear imaging approach for dielectric objects buried under a rough surface," *IEEE Transactions on Geoscience and Remote Sensing,* vol. 52, no. 5, pp. 3013-3022, 2014.

[10] L. L. Monte, D. Erricolo, F. Soldovieri, and M. C. Wicks, "Radio frequency tomography for tunnel detection," *IEEE Transactions on Geoscience and Remote Sensing,* vol. 48, no. 3, pp. 1128-1137, 2010.

[11] X. Song, S. Zhou, and P. Willett, "Reducing the waveform cross correlation of MIMO radar with space–time coding," *IEEE Transactions on Signal Processing,* vol. 58, no. 8, pp. 4213-4224, 2010.

[12] Y. Alvarez *et al.*, "Fourier-based imaging for multistatic radar systems," *IEEE Transactions on Microwave Theory and Techniques,* vol. 62, no. 8, pp. 1798-1810, 2014.

[13] D. Colton and R. Kress, *Inverse acoustic and electromagnetic scattering theory*. Springer Science & Business Media, 2012.

[14] M. Bevacqua, L. Crocco, L. D. Donato, T. Isernia, and R. Palmeri, "Exploiting sparsity and field conditioning in subsurface microwave imaging of nonweak buried targets," *Radio Science,* vol. 51, no. 4, pp. 301-310, 2016.

[15] E. Pettinelli, A. Di Matteo, E. Mattei, L. Crocco, F. Soldovieri, J. D. Redman, A. P. Annan, "GPR response from buried pipes: Measurement on field site and tomographic reconstructions," *IEEE Transactions on Geoscience and Remote Sensing,* vol. 47, no. 8, pp. 2639-2645, 2009.

[16] I. Catapano, L. Crocco, and T. Isernia, "Improved sampling methods for shape reconstruction of 3-D buried targets," *IEEE Transactions on Geoscience and Remote Sensing,* vol. 46, no. 10, pp. 3265-3273, 2008.

[17] S. Sun, B. J. Kooij, and A. G. Yarovoy, "Linearized 3-D electromagnetic contrast source inversion and its applications to half-space configurations," *IEEE Transactions on Geoscience and Remote Sensing,* vol. 55, no. 6, pp. 3475-3487, 2017.

[18] M. T. Bevacqua and T. Isernia, "Boundary Indicator for Aspect Limited Sensing of Hidden Dielectric Objects," *IEEE Geoscience and Remote Sensing Letters,* vol. 15, no. 6, pp. 838-842, 2018.

[19] W. Zhang, A. Hoorfar, and L. Li, "Through-the-wall target localization with time reversal music method," *Progress In Electromagnetics Research,* vol. 106, pp. 75-89, 2010.

[20] M. Ambrosanio and V. Pascazio, "A compressive-sensing-based approach for the detection and characterization of buried objects," *IEEE Journal of Selected Topics in Applied Earth Observations and Remote Sensing,* vol. 8, no. 7, pp. 3386-3395, 2015.

[21] F. Soldovieri, A. Brancaccio, G. Prisco, G. Leone, and R. Pierri, "A Kirchhoff-based shape reconstruction algorithm for the multimonostatic configuration: The realistic case of buried pipes," *IEEE Transactions on Geoscience and Remote Sensing,* vol. 46, no. 10, pp. 3031-3038, 2008.

[22] G. Leone, R. Persico, and R. Solimene, "A quadratic model for electromagnetic subsurface prospecting," *AEU-International Journal of Electronics and Communications,* vol. 57, no. 1, pp. 33-46, 2003.

[23] T. J. Cui, Y. Qin, Y. Ye, J. Wu, G.-L. Wang, and W. C. Chew, "Efficient low-frequency inversion of 3-D buried objects with large contrasts," *IEEE transactions on geoscience and remote sensing,* vol. 44, no. 1, pp. 3-9, 2006.

[24] M. Salucci, L. Poli, N. Anselmi, and A. Massa, "Multifrequency particle swarm optimization for enhanced multiresolution GPR microwave imaging," *IEEE Transactions on Geoscience and Remote Sensing,* vol. 55, no. 3, pp. 1305-1317, 2017.

[25] C. Estatico, A. Fedeli, M. Pastorino, and A. Randazzo, "A Multifrequency Inexact-Newton Method in ${L^ p} $ Banach Spaces for Buried Objects Detection," *IEEE Transactions on Antennas and Propagation,* vol. 63, no. 9, pp. 4198-4204, 2015.

[26] F. Li, Q. H. Liu, and L.-P. Song, "Three-dimensional reconstruction of objects buried in layered media using Born and distorted Born iterative methods," *IEEE Geoscience and Remote Sensing Letters,* vol. 1, no. 2, pp. 107-111, 2004.

[27] V. Pascazio and G. Ferraiuolo, "Statistical regularization in linearized microwave imaging through MRF-based MAP estimation: hyperparameter estimation and image computation," *IEEE transactions on image processing,* vol. 12, no. 5, pp. 572-582, 2003.

[28] M. A. Figueiredo, R. D. Nowak, and S. J. Wright, "Gradient projection for sparse reconstruction: Application to compressed sensing and other inverse problems," *IEEE Journal of selected topics in signal processing,* vol. 1, no. 4, pp. 586-597, 2007.

[29] M. Ndoye, J. M. Anderson, and D. J. Greene, "An MM-Based algorithm for l1-regularized least-squares estimation with an application to ground penetrating radar image reconstruction," in *IEEE Trans. Image. Proc*, 2016.

[30] X. Tan, W. Roberts, J. Li, and P. Stoica, "Sparse learning via iterative minimization with application to MIMO radar imaging," *IEEE Transactions on Signal Processing,* vol. 59, no. 3, pp. 1088-1101, 2011.